

015577

RSS Tech. Report 123196

Issued: December 31, 1996

SSM/I and ECMWF Wind Vector Comparison

Frank J. Wentz

Remote Sensing Systems, Santa Rosa, California

Peter D. Ashcroft

Remote Sensing Systems, Santa Rosa, California

Prepared for:

EOS Project

Goddard Space Flight Center

National Aeronautics and Space Administration

Greenbelt MD 20771

CONTRACT NASW-4714

Prepared by:

Remote Sensing Systems

1101 College Ave., Suite 220, Santa Rosa, CA 95404

(707) 545-2904



Introduction

Wentz [1992] was the first to convincingly show that satellite microwave radiometers have the potential to measure the oceanic wind vector. The most compelling evidence for this conclusion was the monthly wind vector maps derived solely from a statistical analysis of SSM/I observations. In a qualitative sense, these maps clearly showed the general circulation over the world's oceans. In this report we take a closer look at the SSM/I monthly wind vector maps and compare them to ECMWF wind fields. This investigation leads both to an empirical comparison of SSM/I calculated wind vectors with ECMWF wind vectors, and to an examination of possible reasons that the SSM/I calculated wind vector direction would be inherently more reliable at some locations than others.

Computation of SSM/I Wind Vector Maps

The SSM/I wind vector maps are computed somewhat differently than was described in *Wentz* [1992]. The new SSM/I geophysical retrieval algorithm [*Wentz*, 1997] computes a wind direction indicator ΔT_B along with the standard wind speed, water vapor, cloud water and rain products. This new parameter varies with wind speed and wind direction as

$$\Delta T_B = A(W) \cos(\phi - \phi_w)$$

where ϕ is the SSM/I observation azimuth, ϕ_w is the wind direction in the meteorological sense, and the amplitude A varies with wind speed W . An upwind observation is when the wind is blowing towards the SSM/I, i.e., $\phi = \phi_w$. The amplitude of the harmonic variation increases approximately linearly with wind speed.

Determination of the wind direction requires that observations of ΔT_B for the same ocean area be taken from various azimuth directions. Since SSM/I is a single-look sensor, it is not possible to uniquely determine ϕ_w from a single overpass. Furthermore, the wind direction signal is weak (≈ 1 K), so there is a signal-to-noise problem for a single observation. However, by combining observations from many satellite overpasses of the same ocean area, one obtains multiple azimuth looks as well as an improvement in the signal-to-noise by averaging observations. (Note, information on the line-of-sight wind component can be deduced from individual observations.)

We collect all SSM/I observations for a month that fall within a $5^\circ \times 10^\circ$ bin over the ocean. Each bin contains observations over a wide range of azimuth angles. The azimuth angles for the descending orbit segments range from 120° to 220° , and the angles from the ascending segments range for -40° to 60° .

Typically a given bin contains about 30,000 multichannel observations. We understand that $5^{\circ} \times 10^{\circ}$ is a very coarse resolution for science applications, but we chose this as a starting point for this study. Future studies will address results at higher spatial resolutions.

A simple first harmonic analysis is then done for the binned values of ΔT_B . The buoy analysis done by *Wentz* [1992] indicates that the amplitude A varies linearly with W : $A = 0.1W$, where W is in units of meter/second and A is in units of Kelvin. Using this relationship, the above equation can be written as

$$\begin{aligned}\Delta T_B &= 0.1 (W \cos \phi_W \cos \phi + W \sin \phi_W \sin \phi) \\ &= 0.1 (u \cos \phi + v \sin \phi)\end{aligned}$$

where u and v are the zonal and meridional components of the wind. Thus a simple first-order harmonic analysis of the monthly binned ΔT_B values yields the monthly averaged u and v components of the wind.

Calculated Wind Vector Comparison

The monthly and annual SSM/I wind vector estimates are compared to ECMWF estimates from 1992 to 1995. Only the SSM/I on the F10 satellite is used in this analysis. The higher resolution ECMWF maps are first averaged to match the $5^{\circ} \times 10^{\circ}$ resolution of the SSM/I data. In effect, the ECMWF estimates are used as truth to evaluate the accuracy of the SSM/I based estimates. The SSM/I wind direction algorithm is not considered reliable for wind speeds less than 3 m/s, and consequently no results are reported for these low winds. For the sake of visual clarity, ECMWF wind vectors corresponding to speeds less than 2 m/s are not shown in the annual and monthly figures that follow.

Annually averaged wind

Over the 1992–1995 time period, some regions are consistently well estimated, while others were not. As suggested by the annual averages of Figure 1 through Figure 4, the Westerlies blowing around Antarctica are generally well estimated for every month of all years. Thus, this agreement is notable both for its spatial coherence and temporal consistency. Examination of the difference between the SSM/I wind vectors and the ECMWF wind vectors reveals that the residual in this region has no consistent bias.

In contrast to these regions for which the wind direction is consistently and accurately estimated using SSM/I, the estimated wind vector exhibits a *significant and consistent bias* near the West coast of South America and the West coast of Africa. These two regions are also notable for a strong diurnal cycle of cloud water. As is discussed below, diurnal changes can alias into an

ascending versus descending bias, and such a bias will produced a systematic bias in the SSM/I wind direction. Although this coincidence suggests that the diurnal water cycle might be responsible for the inaccurate estimation of wind direction, the link is still somewhat speculative.

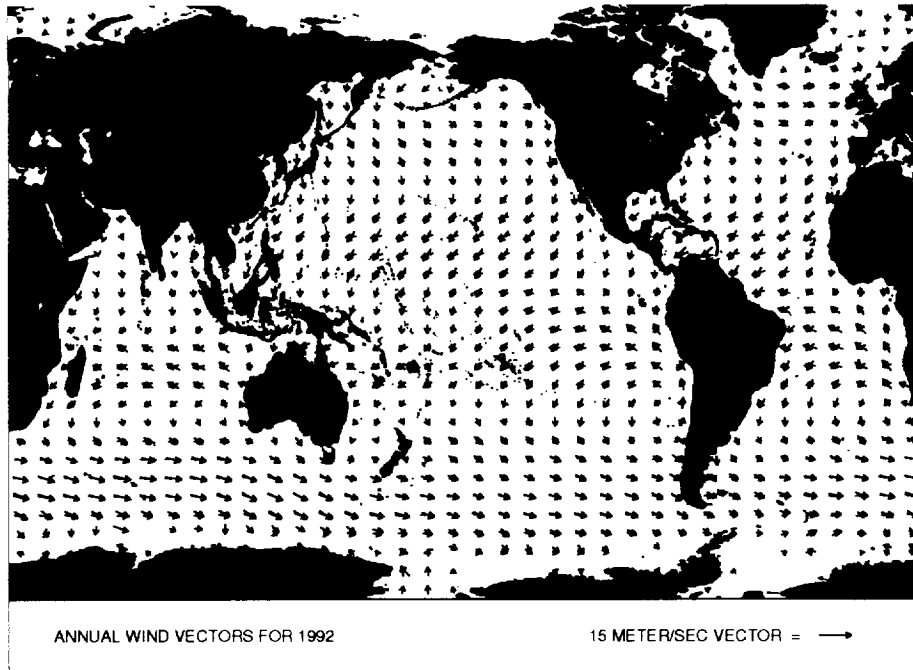


Figure 1: 1992 annually averaged wind vectors as estimated by SSM/I and by ECMWF. Red arrows indicate ECMWF estimates, and black arrows indicate SSM/I estimates.

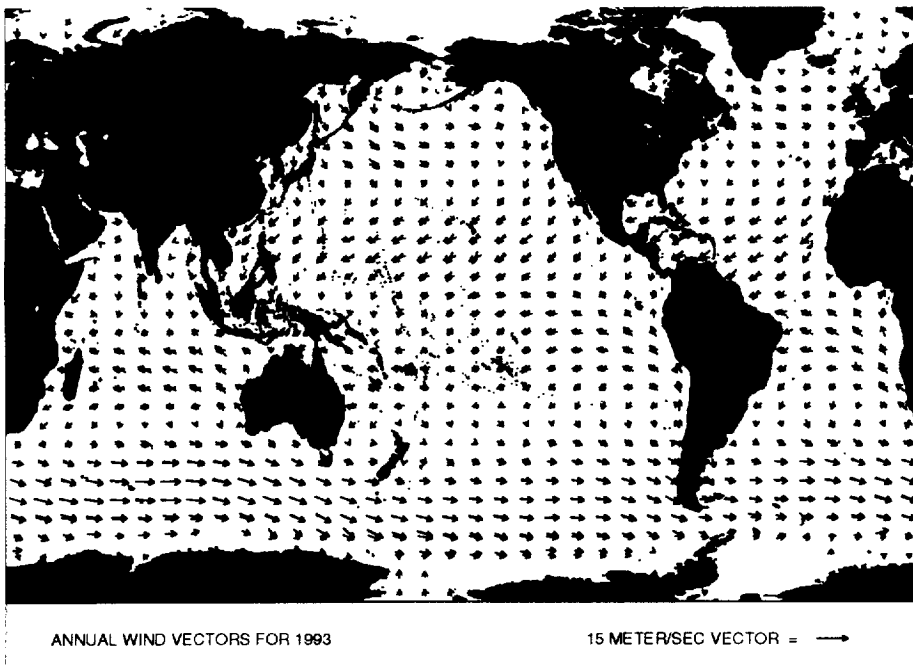


Figure 2: 1993 annually averaged wind vectors as estimated by SSM/I and by ECMWF. Red arrows indicate ECMWF estimates, and black arrows indicate SSM/I estimates.

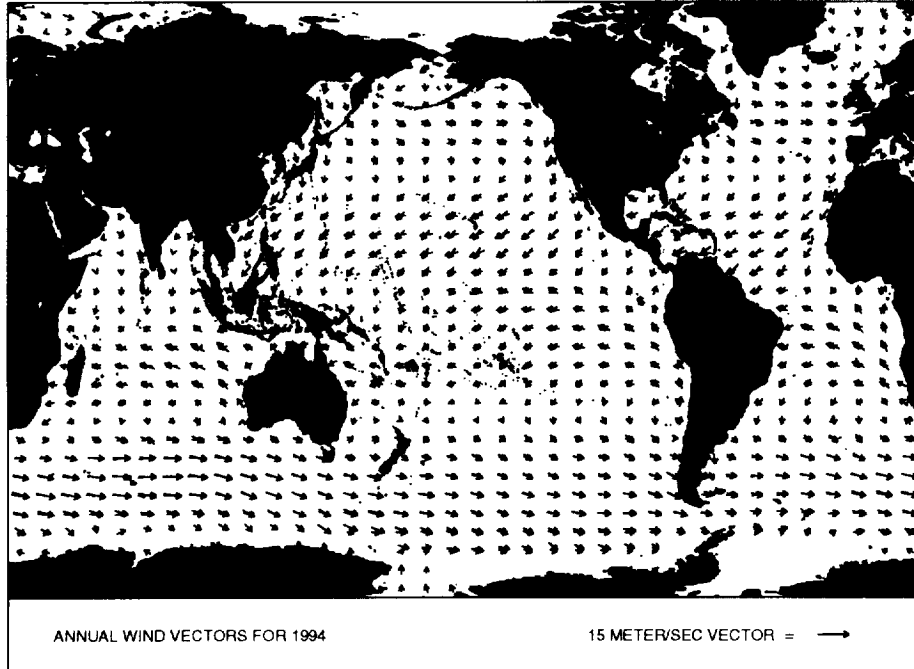


Figure 3: 1994 annually averaged wind vectors as estimated by SSM/I, and by ECMWF. Red arrows indicate ECMWF estimates, and black arrows indicate SSM/I estimates.

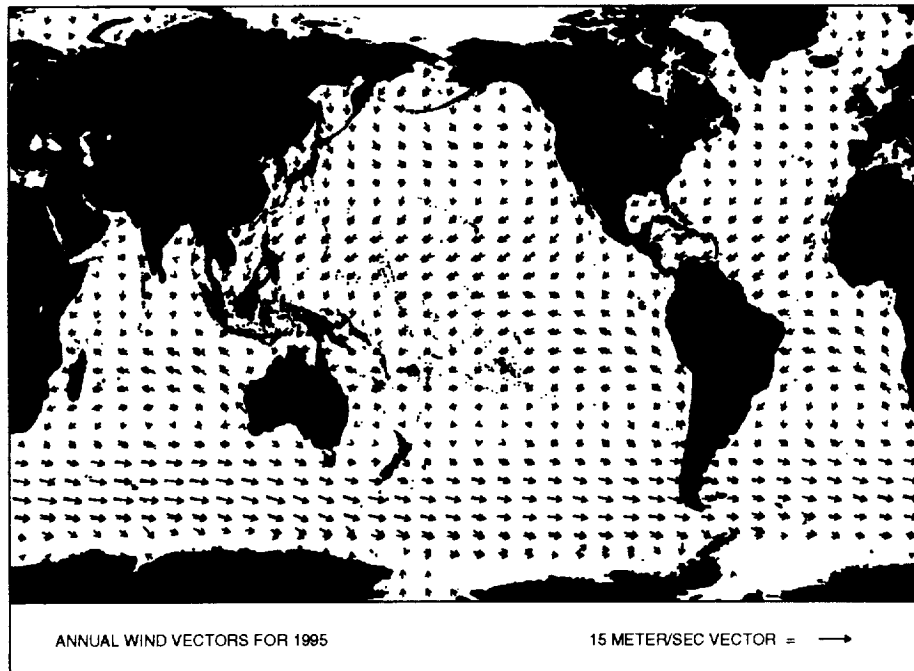


Figure 4: 1995 annually averaged wind vectors as estimated by SSM/I, and by ECMWF. Red arrows indicate ECMWF estimates, and black arrows indicate SSM/I estimates.

Monthly averaged wind

The patterns of the annually averaged wind vectors are also somewhat evident among the monthly data. A typical example of such monthly data is shown in Figure 5 for November 1993. Similar maps corresponding to other months can be found in the Appendix.

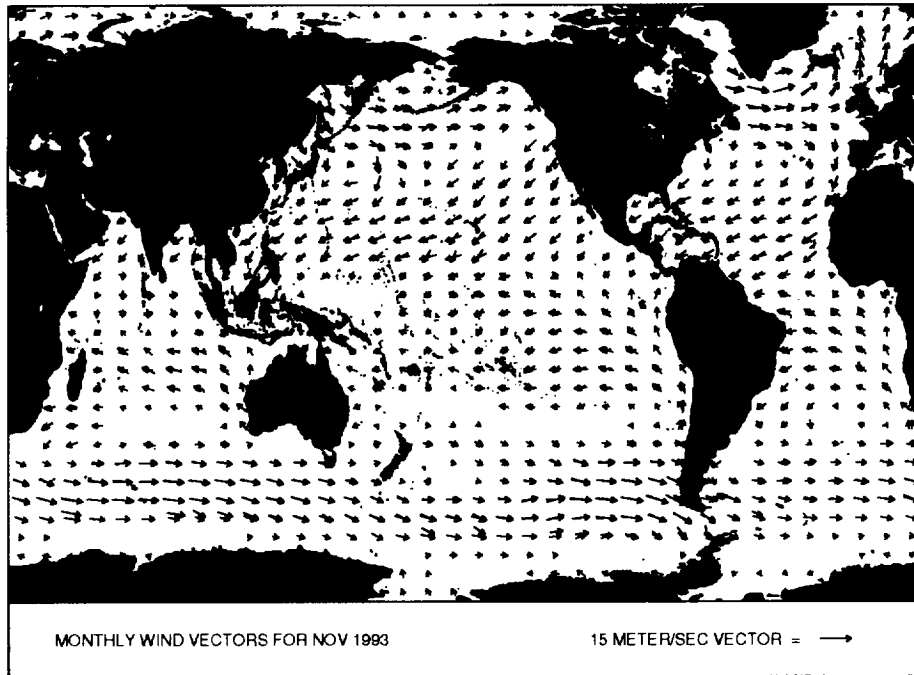


Figure 5: Monthly averaged wind vectors as estimated by SSM/I, and by ECMWF. Red arrows indicate ECMWF estimates, and black arrows indicate SSM/I estimates.

The differences between the SSM/I and ECMWF wind vector estimates for this example month are shown in Figure 6. (The differences is not computed for those locations lacking an SSM/I wind estimate.) This difference plot reveals that some of the regions with the strongest winds according to the ECMWF estimates, (e.g., in the North Atlantic and around Antarctica), are also the most accurately estimated by the SSM/I algorithm. Conversely, some of the regions with the most pronounced and spatially extensive error fields correspond to areas in which the wind is not particularly strong.

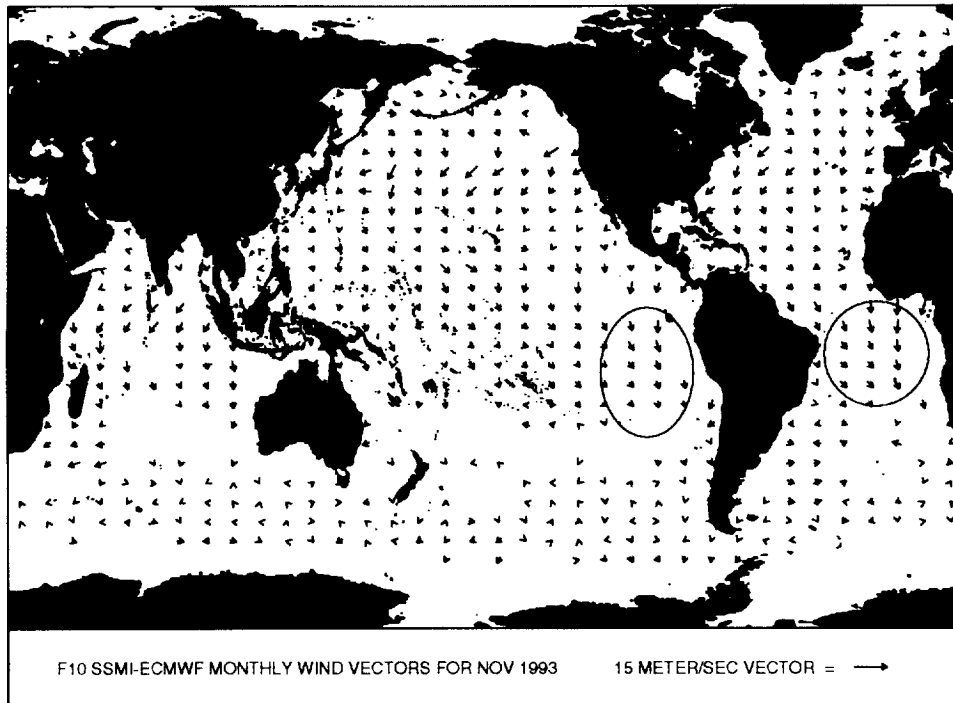


Figure 6: Difference of monthly averaged wind vectors as estimated by SSM/I, and by ECMWF.

The regionally coherent pattern of south pointing difference vectors highlighted in Figure 6 by the red ellipses is also evident in each of the other monthly averages and the yearly averages. As suggested earlier, this might be the result of a strong diurnal cloud water cycle. If the geophysical retrieval algorithm is not completely removing this diurnal signal from ΔT_B , then there will be a slight difference in ΔT_B for the ascending versus descending orbit segments, which will translate into an angular bias in the estimated wind vector. This possibility is investigated and is found plausible through a simple numerical experiment. For a bias of $\pm 30\%$ in ΔT_B , an Easterly wind would acquire a directional error of approximately 20° .

In addition to those errors or biases that are consistent over all the months examined, a number of patterns are quite pronounced for only several months before vanishing. For example, the SSM/I estimates exhibit a spatially coherent bias extending from high Northern latitudes to South of the Equator in both the Atlantic and Pacific oceans for the months of March through August of 1992. Of this extensive region, only that portion indicated by the red ellipses persists throughout the year. A Southward directed spatially coherent bias is also evident in the Indian Ocean over the period from March to August 1992.

The difference vectors for all the months of each year are shown in Figure 7 through Figure 10. These scatter plots generally indicate that the variance of

error in the North-South direction is comparable to that in the East-West direction. In other words, the scatter patterns are roughly circular (although with some offset). On the basis of this evidence, neither of the two directions is more accurately estimated than the other. Another characteristic of these scatter plots is a consistent bias in the South direction (meaning that the North wind component of the SSM/I estimates is too large). As mentioned above, there is the possibility that ascending versus descending biases may be introducing an artificial north component to the SSM/I estimates.

Figure 11 through Figure 18 depict the same information as Figure 7 through Figure 10, but stratified according to the magnitude of the SSM/I wind vector. The first set of figures show the results for winds below 7 m/s, and the second set shows the results for winds above 7 m/s. Generally speaking, the high wind results show less variance and less bias than the low wind results.

Another description of the directional accuracy of SSM/I wind vectors for the four years of comparison is provided in Table 1 through Table 4. These tables clearly show that the accuracy increases as the wind speed (ECMWF) increases. For 8 m/s and above the rms wind direction error is 20°, or less. Thus at the higher winds, the wind direction signal (i.e., ΔT_B) is sufficiently strong to obtain a reliable estimate of the monthly averaged wind vector.

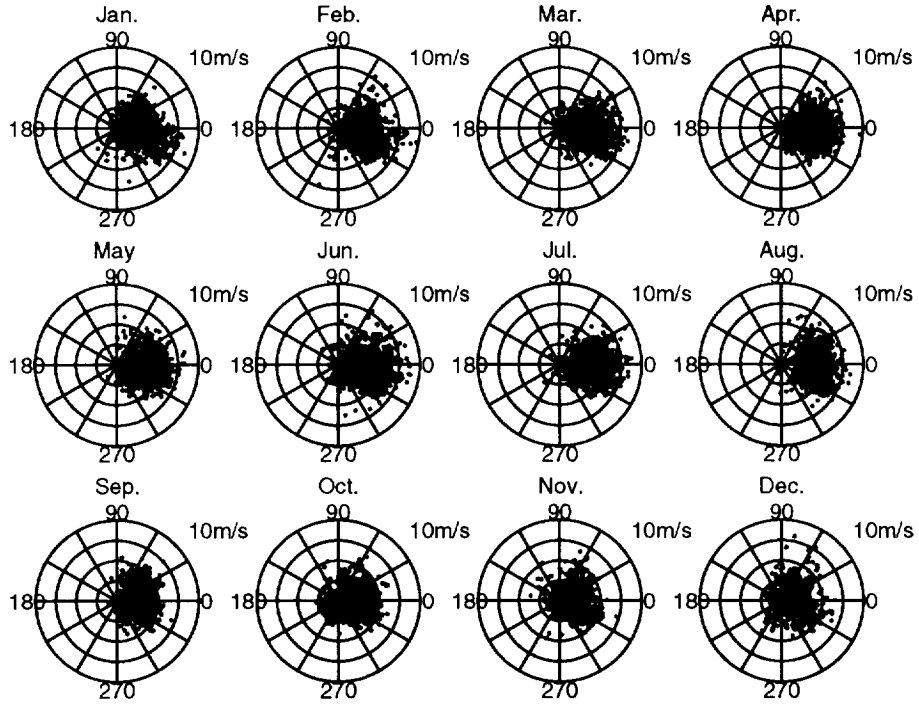


Figure 7: SSM/I-ECMWF wind vectors for each month of 1992. 0° corresponds to a vector out of the North. Outermost ring is 10 m/s for each.

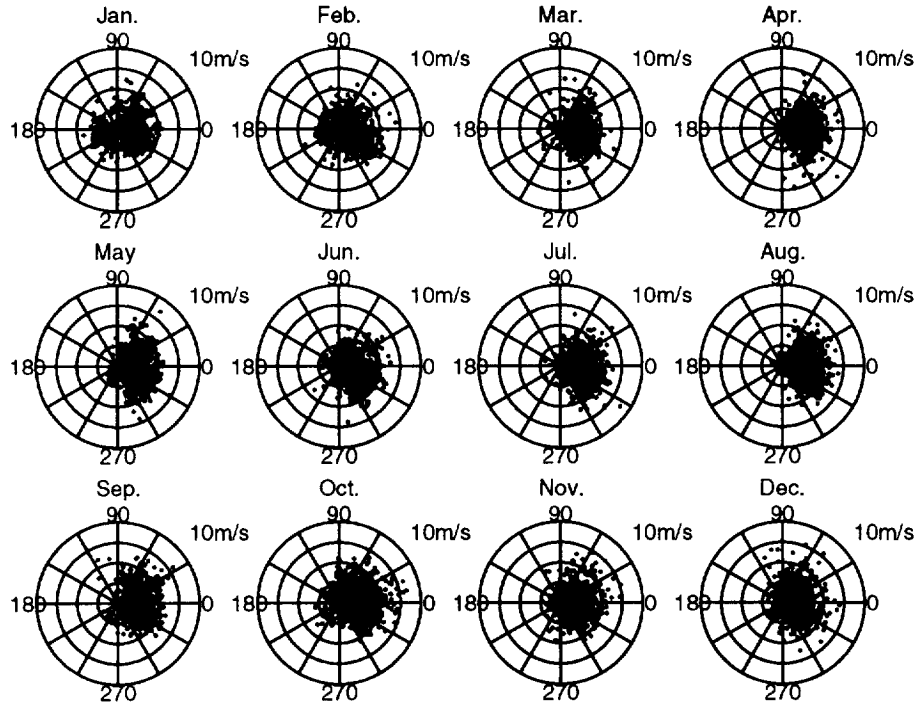


Figure 8: SSM/I-ECMWF wind vectors for each month of 1993. 0° corresponds to a vector out of the North. Outermost ring is 10 m/s for each.

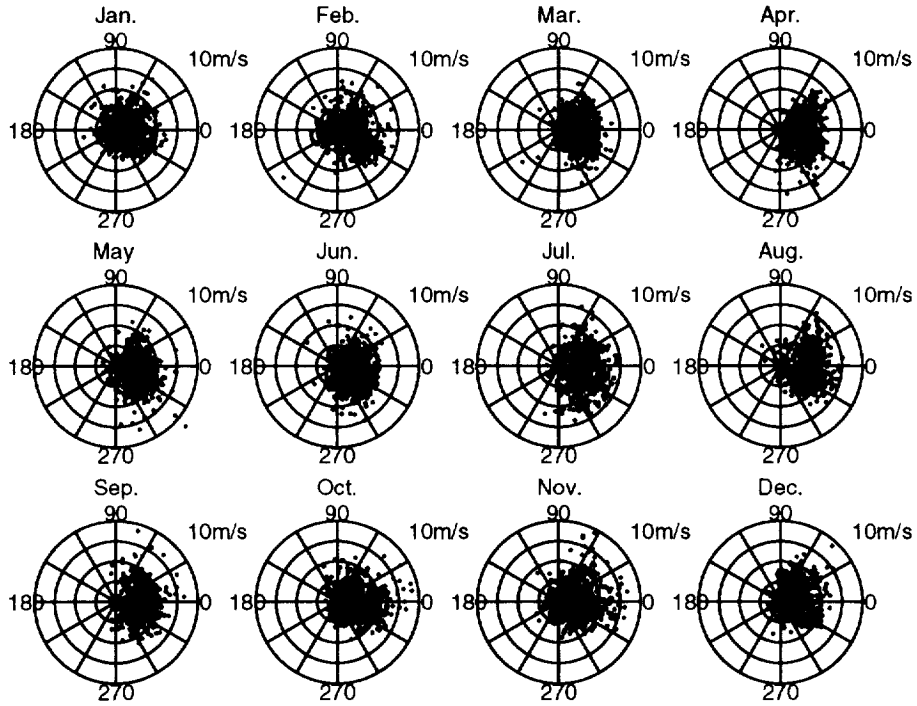


Figure 9: SSM/I-ECMWF wind vectors for each month of 1994. 0° corresponds to a vector out of the North. Outermost ring is 10 m/s for each.

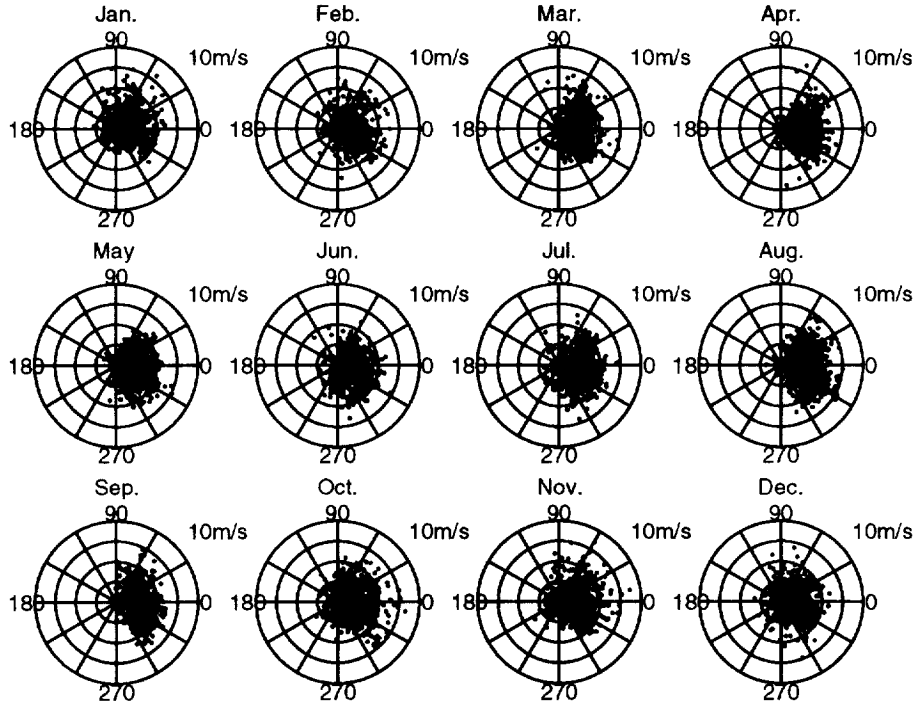


Figure 10: SSM/I-ECMWF wind vectors for each month of 1995. 0° corresponds to a vector out of the North. Outermost ring is 10 m/s for each.

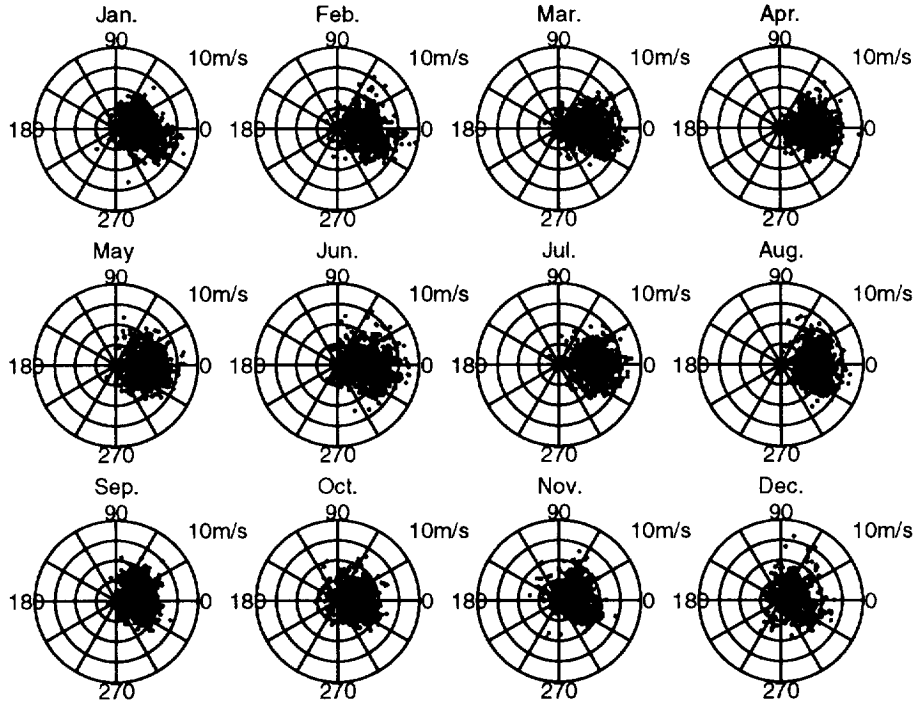


Figure 11: SSM/I-ECMWF wind vectors for each month of 1992 for cases in which the magnitude of SSM/I was less than 7 m/s. 0° corresponds to a vector out of the North. Outermost ring is 10 m/s for each.

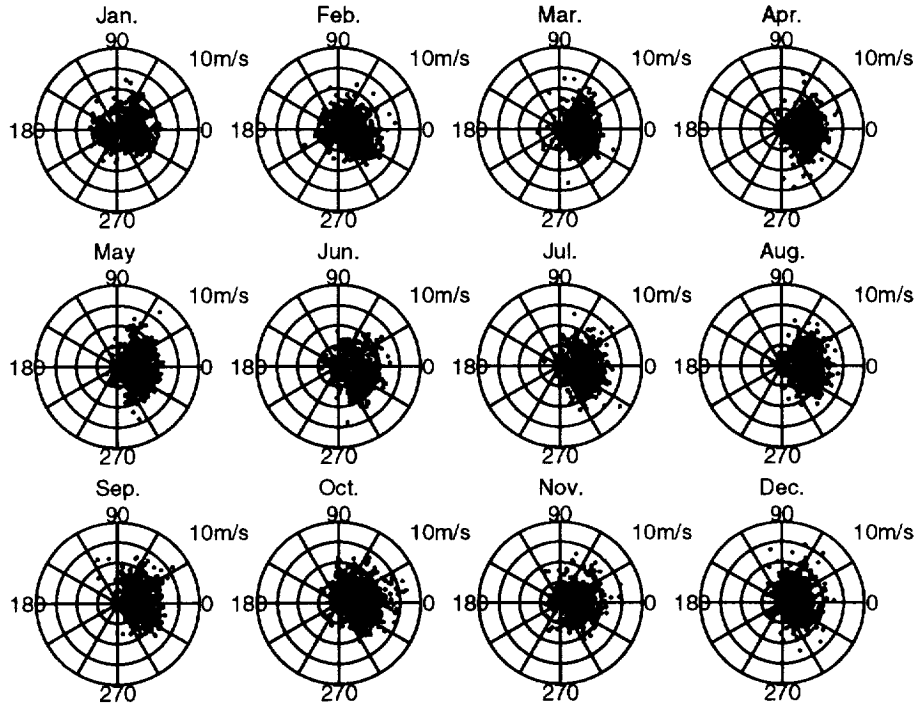


Figure 12: SSM/I-ECMWF wind vectors for each month of 1993 for cases in which the magnitude of SSM/I was less than 7 m/s. 0° corresponds to a vector out of the North. Outermost ring is 10 m/s for each.

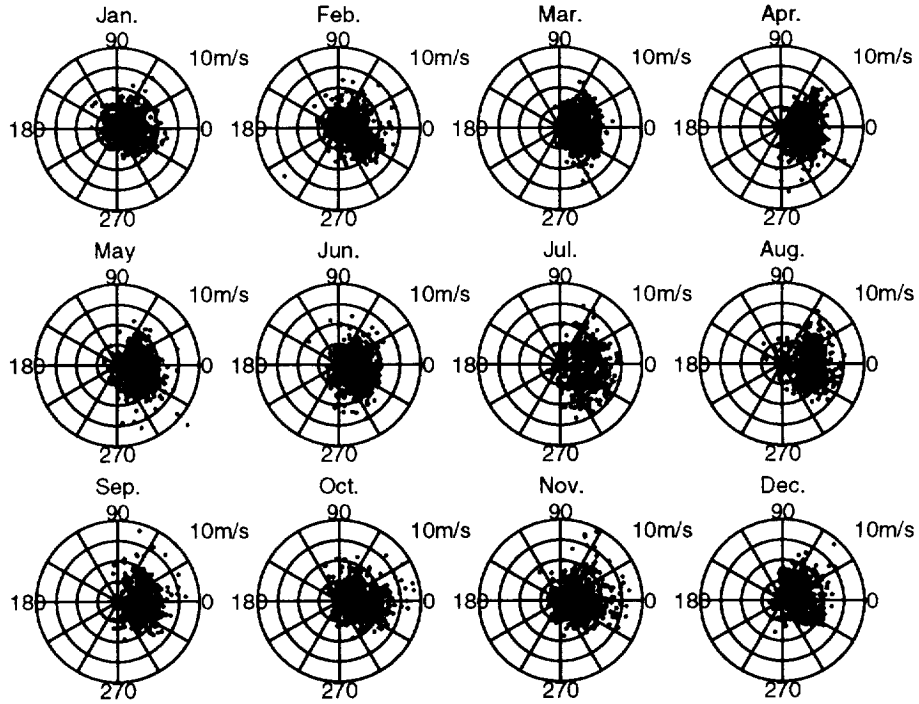


Figure 13: SSM/I-ECMWF wind vectors for each month of 1994 for cases in which the magnitude of SSM/I was less than 7 m/s. 0° corresponds to a vector out of the North. Outermost ring is 10 m/s for each.

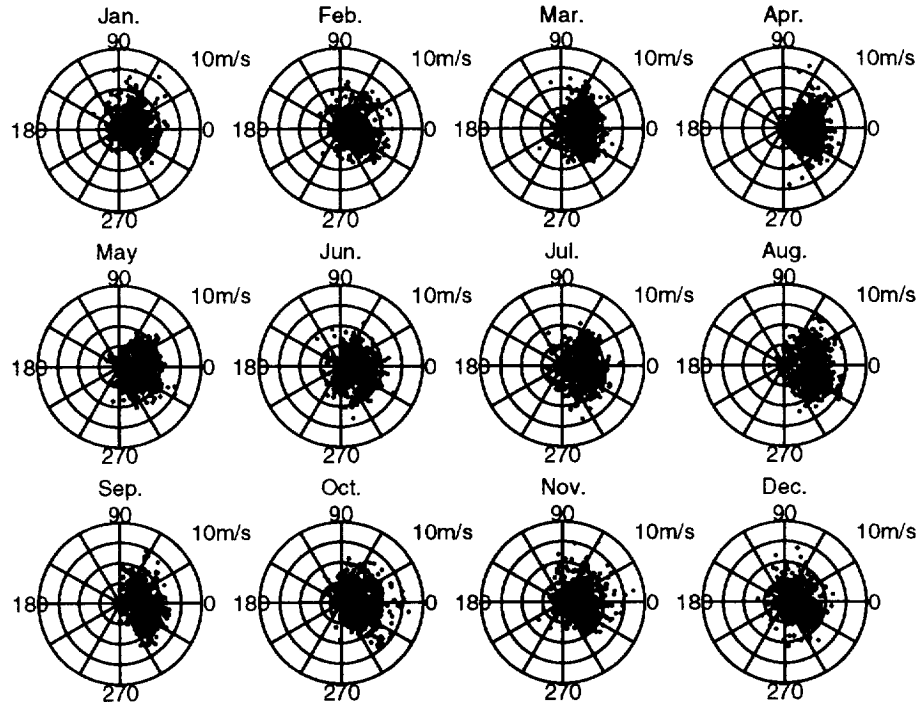


Figure 14: SSM/I-ECMWF wind vectors for each month of 1995 for cases in which the magnitude of SSM/I was less than 7 m/s. 0° corresponds to a vector out of the North. Outermost ring is 10 m/s for each.

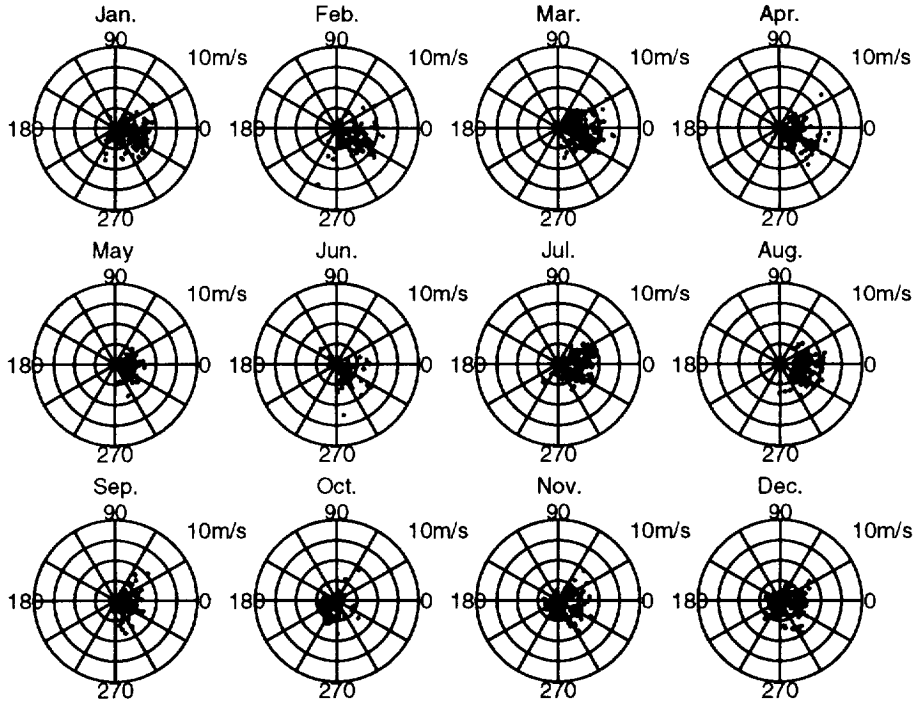


Figure 15: SSMI-ECMWF wind vectors for each month of 1992 for cases in which the magnitude of SSM/I was greater than 7 m/s. 0° corresponds to a vector out of the North. Outermost ring is 10 m/s for each.

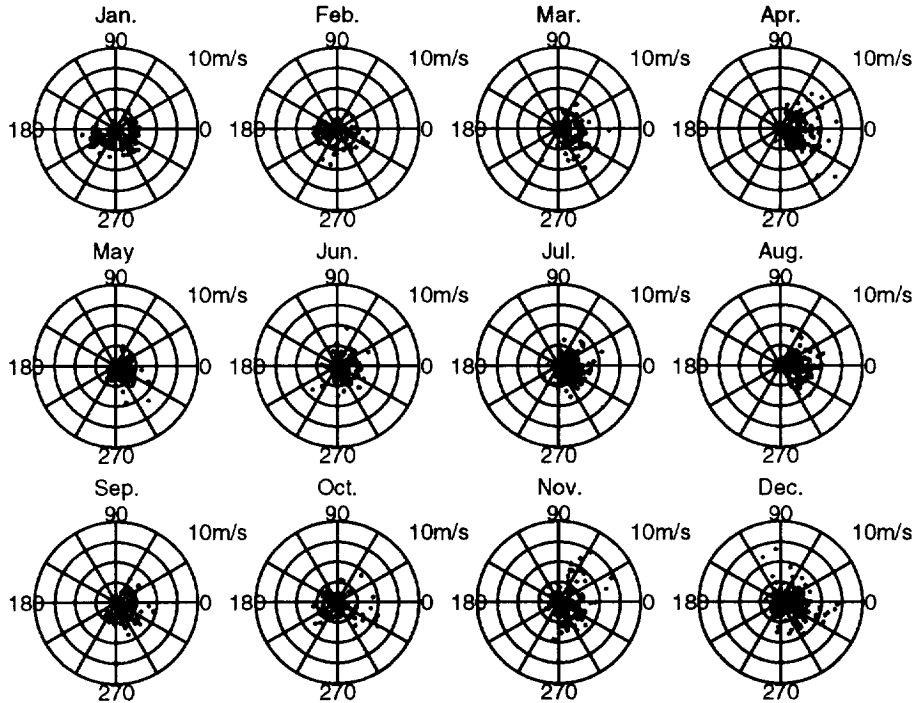


Figure 16: SSMI-ECMWF wind vectors for each month of 1993 for cases in which the magnitude of SSM/I was greater than 7 m/s. 0° corresponds to a vector out of the North. Outermost ring is 10 m/s for each.

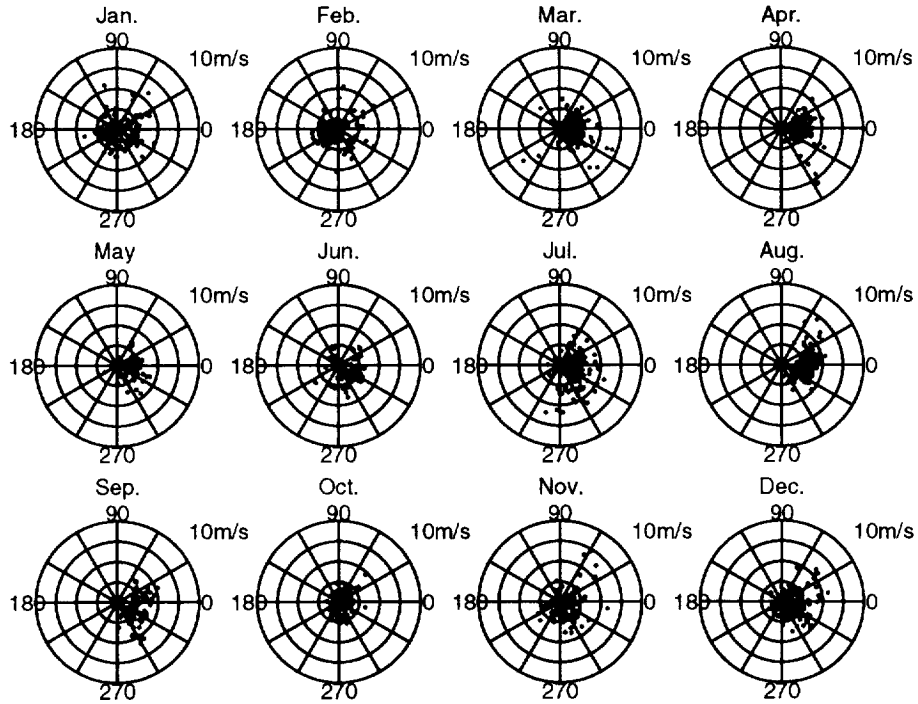


Figure 17: SSM/I-ECMWF wind vectors for each month of 1994 for cases in which the magnitude of SSM/I was greater than 7 m/s. 0° corresponds to a vector out of the North. Outermost ring is 10 m/s for each.

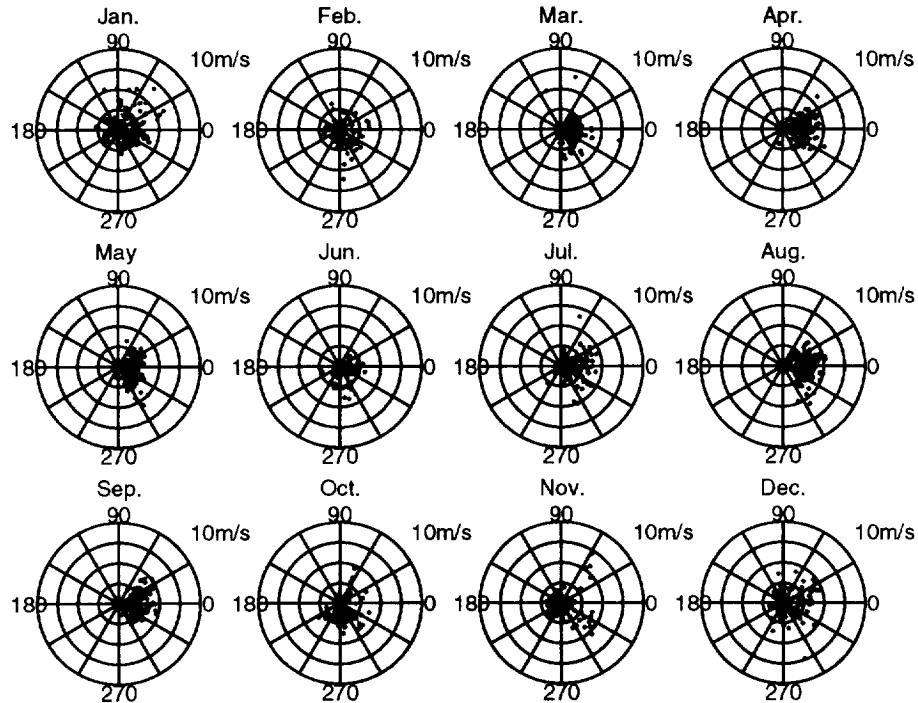


Figure 18: SSM/I-ECMWF wind vectors for each month of 1995 for cases in which the magnitude of SSM/I was greater than 7 m/s. 0° corresponds to a vector out of the North. Outermost ring is 10 m/s for each.

Table 1. Mean error and RMS range of error for direction of 1992 SSM/I wind vector estimates.

ECMWF Speed	N	mean (deg.)	rms (deg.)
0	84	15.3	95.7
1	675	-7.7	97.7
2	960	-0.4	84.6
3	1065	-2.3	71.4
4	1183	-11.7	57.6
5	1061	-21.5	48.7
6	928	-19.7	40.0
7	684	-13.8	32.3
8	377	-1.2	21.0
9	148	0.7	17.4
10	38	7.6	8.8
11	11	10.9	5.0
12	2	10.6	2.6
Overall	7227	-9.9	63.3

Table 2. Mean error and RMS range of error for direction of 1992 SSM/I wind vector estimates.

ECMWF Speed	N	mean (deg.)	rms (deg.)
0	69	19.1	108.7
1	502	1.5	87.4
2	810	-3.5	73.4
3	856	-6.8	55.4
4	1011	-10.7	47.9
5	993	-17.2	38.3
6	907	-16.9	29.9
7	658	-10.6	25.0
8	419	-4.2	18.9
9	296	0.2	14.9
10	117	4.5	10.0
11	30	8.9	6.4
12	3	8.0	2.1
13	2	10.9	3.0
Overall	6680	-8.6	50.8

Table 3. Mean error and RMS range of error for direction of 1995 SSM/I wind vector estimates.

ECMWF Speed	N	mean (deg.)	rms (deg.)
0	66	2.0	97.7
1	454	-1.9	91.0
2	736	-3.1	75.7
3	816	-1.9	61.7
4	1001	-8.0	52.2
5	1027	-15.6	44.4
6	901	-18.0	33.3
7	769	-12.5	26.5
8	462	-4.7	21.9
9	255	-0.4	18.7
10	132	7.7	11.5
11	46	9.6	9.5
12	6	3.4	4.9
13	4	-0.9	1.6
Overall	6681	-8.3	52.8

Table 4. Mean error and RMS range of error for direction of 1995 SSM/I wind vector estimates.

ECMWF Speed	N	mean (deg.)	rms (deg.)
0	54	19.0	88.9
1	395	2.5	81.3
2	624	5.0	68.5
3	777	-4.0	57.7
4	856	-8.6	45.1
5	966	-12.9	38.6
6	960	-14.8	32.3
7	743	-8.0	25.9
8	428	-0.2	18.7
9	238	2.0	13.7
10	103	8.7	10.4
11	30	10.7	8.2
12	8	12.8	5.2
13	2	10.6	3.0
Overall	6190	-5.9	47.2

Conclusions and Remaining Questions

For wind of 8 m/s and above, the monthly averaged SSM/I wind vectors are in good agreement ($\pm 20^\circ$) with the ECMWF wind fields. However at lower winds, the disagreement is large due to the wind direction T_B signal becoming small (< 0.5 K). Biases between ascending and descending SSM/I orbit segments are probably responsible for some of the observed error.

The possibility exists that by using additional SSM/I's (F11 and F13) more accurate wind vector retrievals could be obtained. Also, analyses using smaller spatial and temporal resolutions should be done. The advantage to estimating the wind direction over a shorter period and smaller area is that the wind will be more consistent, but the disadvantage is that the number of observations available near a given location will be smaller. Also, the problem of an ascending versus descending T_B bias should be examined with an eye towards remove the bias and thereby improving the retrieved wind vectors.

Even though the scientific utility of SSM/I wind vector maps is still questionable, the results herein do provide further evidence that satellite microwave radiometers can measure the ocean wind vector. The 20° wind direction accuracy for winds of 8 m/s and above is remarkable considering the fact that SSM/I was never intended to measure wind direction. We are very pleased that NASA is planning to fly a 2-look, polarimetric radiometer as part of the SeaWinds-2 Mission. The combined SeaWinds-2 radiometer/scatterometer will be the ideal sensor complement for measuring the oceanic wind field.

References

- Wentz, F.J., Measurement of Oceanic Wind Vector Using Satellite Microwave Radiometers, *IEEE Transactions on Geoscience and Remote Sensing*, 30 (5), 960-972, 1992.
- Wentz, F.J., A Well Calibrated Ocean Algorithm for SSM/I, *Journal of Geophysical Research*, In Press, 1997.

Appendix to Report

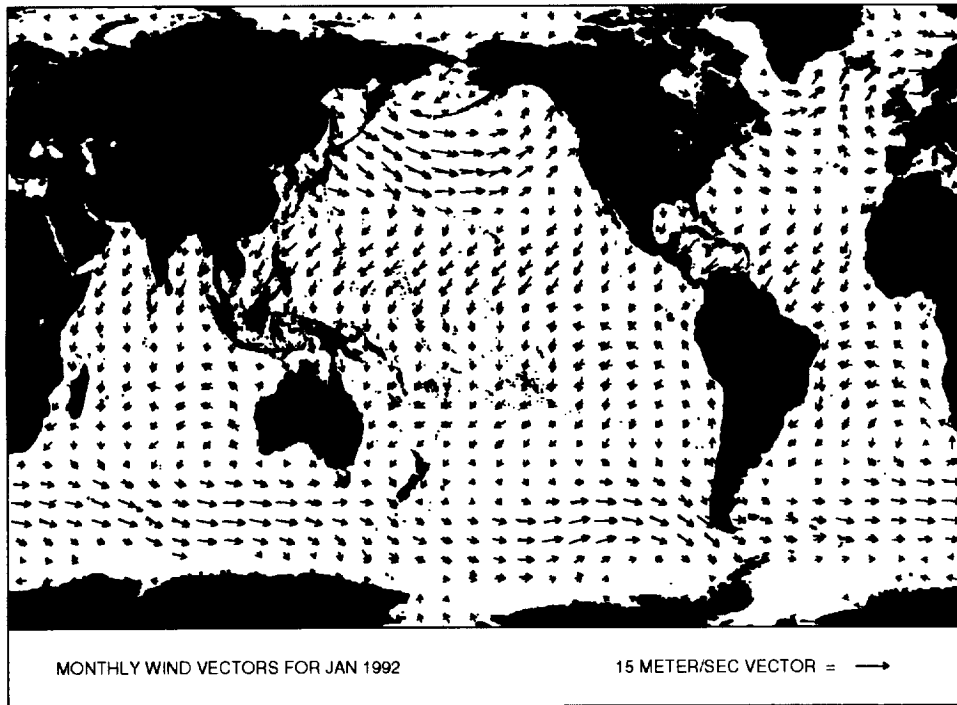


Figure 1: Monthly averaged wind vectors. Red arrows indicate ECMWF estimates, and black arrows indicate SSM/I estimates.

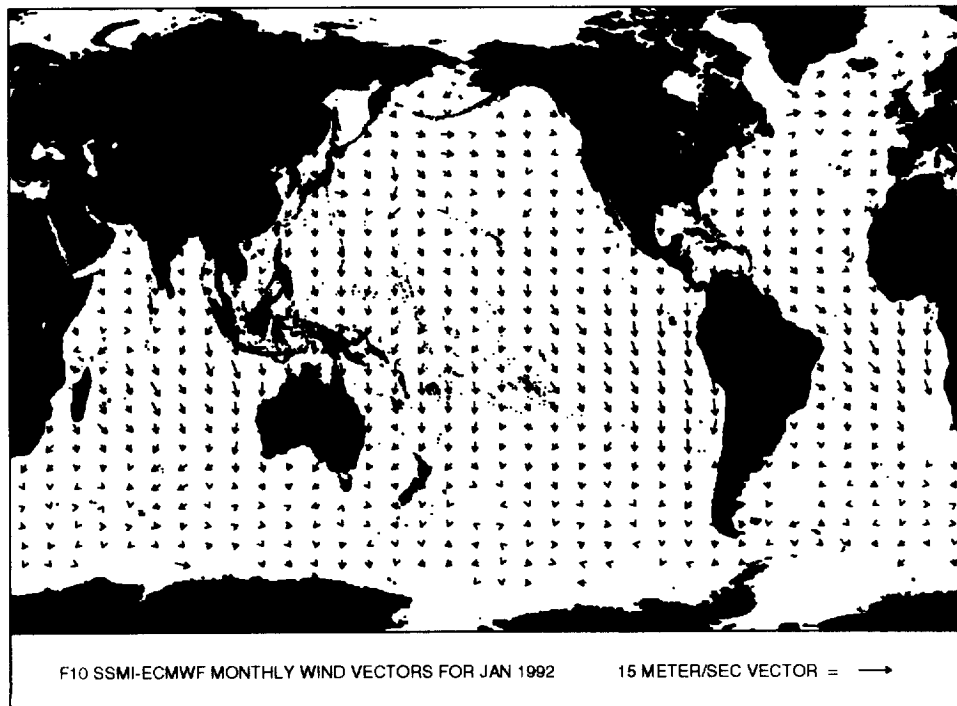


Figure 2: Difference of monthly averaged wind vectors estimated by SSM/I and by ECMWF.

